Climate signals in stable carbon and hydrogen isotopes of lignin methoxy groups from southern German beech trees

Anna Wieland[1], Markus Greule[1], Philipp Roemer[2], Jan Esper[2,3], and Frank Keppler[1,4]

[1]Institute of Earth Sciences, Heidelberg University, Im Neuenheimer Feld 234-236, 69120 Heidelberg, Germany
5 [2]Department of Geography, Johannes Gutenberg University Mainz, 55128 Mainz, Germany
[3]Global Change Research Institute of the Czech Academy of Sciences (CzechGlobe), 60300 Brno, Czech Republic
[4]Heidelberg Center for the Environment (HCE), Heidelberg University, 69120 Heidelberg, Germany

Correspondence to: Frank Keppler (frank.keppler@geow.uni-heidelberg.de) and Anna Wieland (anna.wieland@geow.uni-
10 heidelberg.de)

Abstract. Stable hydrogen and carbon isotope ratios of wood lignin methoxy groups ($\delta^{13}C_{LM}$ and $\delta^{2}H_{LM}$ values) have been shown to be reliable proxies of past temperature variations. Previous studies showed that $\delta^{2}H_{LM}$ values even work in temperate environments where classical tree-ring width and maximum latewood density measurements are less skilful. Here, we analyse annually resolved $\delta^{13}C_{LM}$ values from 1916-2015 of four beech trees (*Fagus sylvatica*) from a temperate site near 15 Hohenpeißenberg in southern Germany and compare these data with regional to continental scale climate observations. Initial $\delta^{13}C_{LM}$ values were corrected for the Suess effect (a decrease of $\delta^{13}C$ in atmospheric CO_2) and physiological tree responses to increasing atmospheric CO_2 concentrations considering a range of published discrimination factors. The calibration of $\delta^{13}C_{LM}$ chronologies against instrumental data reveals highest correlations with regional summer (r = 0.68) and mean annual temperatures (r = 0.66), as well as previous-year September to current-year August temperatures (r = 0.61), all calculated from 20 1916-2015 and reaching p < 0.001. Additional calibration trials using detrended $\delta^{13}C_{LM}$ values and climate data, to constrain effects of autocorrelation on significance levels, returned $r_{summer} = 0.46$ (p < 0.001), $r_{annual} = 0.25$ (p < 0.05) and $r_{prev.Sep-Aug} = 0.18$ (p > 0.05). The new $\delta^{13}C_{LM}$ chronologies were finally compared with previously produced $\delta^{2}H_{LM}$ values of the same trees to evaluate the additional gain of assessing past climate variability using a dual-isotope approach. Compared to $\delta^{13}C_{LM}$, $\delta^{2}H_{LM}$ values correlates substantially stronger with large-scale temperatures averaged over western Europe ($r_{prev.Sep-Aug} = 0.69$), 25 whereas only weak and mainly insignificant correlations are obtained between precipitation and both isotope chronologies ($\delta^{13}C_{LM}$ and $\delta^{2}H_{LM}$ values). Our results indicate great potential of using $\delta^{13}C_{LM}$ values from temperate environments as a proxy for local temperatures, and in combination with $\delta^{2}H_{LM}$ values, to assess regional to sub-continental scale temperature patterns.

1 Introduction

Trees are a powerful archive in global climate research (Esper et al., 2016, 2018; Ljungqvist et al., 2020) as they endure for 30 centuries in widespread temperate climate zones and form yearly growth rings that can be used to analyze factors influencing wood formation (Stoffel and Bollschweiler, 2008). Weather and climate parameters affect the physiological process within

these tree rings. Thus growth specific parameters, such as ring width, maximum latewood density, and the isotopic composition of bulk wood, cellulose, or lignin have proven to be climate sensitive (Daux et al., 2011; Esper, 2000; Esper et al., 2015; Hafner et al., 2011; Konter et al., 2014; Kress et al., 2010; McCarroll and Loader, 2004; Reynolds-Henne et al., 2007; Treydte et al.,
35 2001; Wang et al., 2011). In addition Greule et al. (2019) and Keppler et al. (2007) showed that stable hydrogen and carbon isotope ratios of wood lignin methoxy groups (δ^2H_{LM} and $\delta^{13}C_{LM}$ values) have great potential to be applied for paleoclimate reconstructions. For a more detailed overview of its applications in paleoclimate research we refer to previous studies by (Anhäuser et al., 2020; Gori et al., 2013; Greule et al., 2021; Hepp et al., 2017; Lee et al., 2019; Van Raden et al., 2013; Wang et al., 2020). The isotopic ratios of these specific chemical moieties (-OCH$_3$ groups) of lignin remain unchanged throughout
40 the lifetime of a tree and thus reflect the methoxy isotopic composition at the time of its biochemical formation (Greule et al., 2008; Keppler et al., 2007). While the traditional methods for analyzing stable isotope ratios of a-cellulose or nitrate cellulose require time-consuming preparation, $\delta^{13}C_{LM}$ and δ^2H_{LM} values can readily be measured as iodomethane (CH$_3$I) upon treatment with hydroiodic acid, providing a fast and straightforward preparation (Greule et al., 2008). Furthermore, the removal of water from bulk wood samples is not necessary as it does not affect the isotope analysis (Greule et al., 2008, 2009). It is also
45 advantageous for isotope analysis that methoxy groups are highly abundant in tree rings as wood contains around 25-30 % of lignin and the proportion of methoxy groups in lignin (on a carbon basis) may reach 20 % (Keppler et al., 2007). Therefore, small sample amounts of only 1 mg and 2.5 mg of bulk wood (milled or in pieces) are required for reliable measurements of $\delta^{13}C_{LM}$ and δ^2H_{LM} values (Greule et al., 2008, 2009). Finally, the analytical procedure for measuring δ^2H_{LM} values was considerably improved by the availability of new reference materials that are in full accordance with the requirements of
50 normalizing stable isotope measurements (Greule et al., 2019, 2020).

Most previous methoxy based research have applied δ^2H_{LM} values for climate studies (Anhäuser et al., 2017a, 2017b, 2020; Greule et al., 2021; Keppler et al., 2007; Riechelmann et al., 2017; Wang et al., 2020). In general, the hydrogen isotopic composition of trees is controlled by its source water, and hence the stable isotopes composition of local precipitation (Sternberg, 2009; Tang et al., 2000). Therefore, the temperature dominated signal in $\delta^2H_{precipitation}$ (Dansgaard, 1964) is reflected
55 in δ^2H_{LM} values as has been demonstrated for mid-latitude sites (Anhäuser et al., 2017a; Greule et al., 2021). A highly significant correlation was documented between δ^2H_{LM} values and mean annual temperatures (MAT), whereas 'shifted' MAT (defined as previous September to recent August) showed the highest coefficients with r = 0.56 (Anhäuser et al., 2020). Wang et al. (2020) found significant correlations between δ^2H_{LM} values and April-August temperatures (r = 0.58 to 0.7) for two coniferous species (*Larix gmelinii*, larch and *Pinus sylvestris* var. *mongolica*, pine) from a permafrost forest in northeastern
60 China. Even higher correlations were reported between beech trees from a low elevation site in southern Germany and west European large-scale temperature changes at r = 0.72 (Anhäuser et al., 2020).

Although there exist some studies (Gori et al., 2013; Mischel et al., 2015; Riechelmann et al., 2016; Wang et al., 2020), less attention has been given to the climate sensitivity of $\delta^{13}C_{LM}$ values. The carbon of each annual tree ring has its origin in the atmospheric CO$_2$. Thus the carbon isotope composition in trees mainly consists of the isotopic values of atmospheric CO$_2$
65 ($\delta^{13}C_{atmos}$), the concentration of atmospheric CO$_2$, and the diffusion and fractionation of $\delta^{13}C$ through stomatal pores (-4.4

mUr) and carbon fixation via the photosynthetic enzyme Rubisco (-27 mUr) (Francey and Farquhar, 1982) (Please note, that we follow the suggestion by Brand and Coplen (2012) and express isotope δ-values in milli-Urey [mUr] (after H.C. Urey, 1948) instead of per mil [‰]). The carbon isotopic composition in trees can be expressed as the deviation between $\delta^{13}C_{atmos}$ and the isotopic discrimination of ^{13}C during carbon diffusion and fixation by plants (Eq. 1) (Keeling et al., 2017):

70 $$\delta^{13}C_{tree} = \delta^{13}C_{atmos} - \left[a + (b-a)\frac{c_i}{c_a} - \frac{(b-a_m)\left(\frac{A}{c_a}\right)}{g_i} - f\Gamma^*/c_a \right] \qquad (1)$$

Where a expresses the fractionation by diffusion through the stomata and b describes the fractionation to carboxylation, while ci reflects the inner leaf CO_2 concentration and ca ambient air CO_2 concentrations (Francey and Farquhar, 1982). The last two terms of Eq. 1 represent the mesophyll and photorespiration effects with a_m the fractionation by dissolution and diffusion from the intercellular air spaces to the sites of carboxylation in the chloroplasts, A the leaf-level gross photosynthesis, g_i the

75 mesophyll conductance, f the discrimination due to photorespiration, and Γ the CO_2 compensation point in the absence of day respiration (Cernusak et al., 2013; Farquhar et al., 1982; Keeling et al., 2017; Seibt et al., 2008). These effects are normally neglected but are necessary for understanding the discrimination changes of ^{13}C due to increasing CO_2 concentration (Seibt et al., 2008). The terms of mesophyll and photorespiration are both negative and their absolute magnitude decrease with increasing c_a, resulting in increasing discrimination with rising CO_2 concentration (Keeling et al., 2017).

80 Since the fractionations due to stomatal conductance and Rubisco (*a* and *b)* are considered constant and the terms of mesophyll and photorespiration are normally negligible, the discrimination of ^{13}C is mainly controlled by the *ci/ca* ratio. If *ci* increases, stomatal control is higher than the rate of photosynthesis. The dominance of stomatal control and photosynthesis rate thereby depends on various environmental factors, including temperature, air humidity, precipitation amount, and seasonality (McCarroll and Loader, 2004). Furthermore, the isotopic fractionation between the photosynthate and cellulose or lignin is

85 assumed to be small (Francey and Farquhar, 1982). Consequently, environmental factors that influence the *ci/ca* ratio are also considered to additionally control $\delta^{13}C_{LM}$ values.

The few studies that applied $\delta^{13}C_{LM}$ values of tree rings already demonstrated a relationship with climate parameters. Wang et al. (2020) and Riechelmann et al. (2016) documented highly significant correlations between $\delta^{13}C_{LM}$ values and mean summer temperatures in high elevation environments. Wang et al. (2020) observed highest correlations with April to August

90 temperatures (r = 0.64) and Riechelmann et al. (2016) with June to August temperatures (r = 0.66). In addition, Gori et al. (2013) report correlations with spring and annual mean temperatures, and Mischel et al. (2015) with August maximum temperatures. However, in all previous studies, non-significant correlations (p > 0.05) were reported with precipitation.

In this study, we evaluate the applicability of $\delta^{13}C_{LM}$ values of trees as a paleoclimate proxy in temperate low elevation environments. Therefore, we measured annually resolved $\delta^{13}C_{LM}$ values of four *Fagus sylvatica* L. trees in southern Germany

95 at Hohenpeißenberg and analyzed the climate sensitivity and non-climatic response (to atmospheric CO_2 changes) of $\delta^{13}C_{LM}$ values. Furthermore, to evaluate the potential of reconstructing past climate variability using dual-isotope approach, we revisit the δ^2H_{LM} values of the same trees provided by Anhäuser et al. (2020). However, these previous data were corrected according to new constraints regarding analytical issues of the isotope measurements of methoxy groups (Greule et al., 2021). Finally,

the dual isotope methoxy measurements of Hohenpeißenberg tree rings were used to critically evaluate their potential as a

100 proxy for regional to sub-continental scale temperature patterns.

2 Material and Methods

2.1 Study site

The study site is located close to the Hohenpeißenberg municipality in southern Germany, where tree samples were collected

from the northeastern slope of the Hoher Peißenberg mountain (47° 48′ N, 11° 01′ E; altitude ~800 m). For a detailed map of

105 the sampling site, we would like to refer the reader to the study by Anhäuser et al. (2020). The region is characterized by a

strong temperature increase, particularly since the 1980s, and insignificant precipitation trends (Fig. 1a). Annual mean

temperatures range from 6.22 °C (1940) to 9.73 °C (2018) and precipitation totals from 788 mm (1943) to 1316 mm (1966).

The seasonal climate is characterized by a distinct precipitation peak in summer including 138 mm (period 1961-1990) in July

(Fig. 1b).
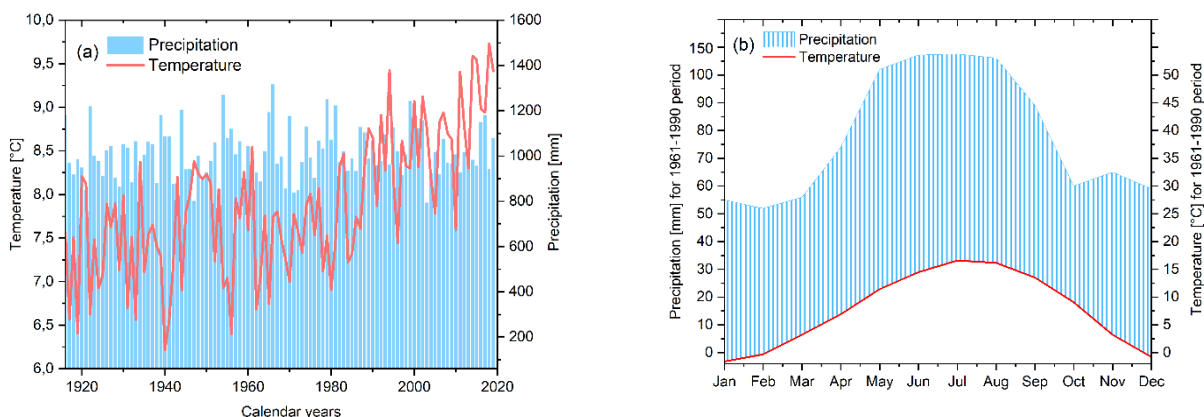
Figure 1. Climate at Hohenpeißenberg. (a) Mean annual temperatures and precipitation totals since 1916, and (b) mean monthly temperatures and precipitation amounts calculated from 1961-1990 (CRU TS 4.04 data at 47.75°N/11.25°E).

110 ### 2.2 Tree samples and $\delta^{13}C_{LM}$ analysis

Four *Fagus sylvatica* trees (F1-F4) were sampled in spring and autumn 2016. The samples were extracted at breast height

(1.2 m above ground) using an increment borer with a diameter of 5 mm. Every tree is represented by two cores, with an age

of each tree back to 1912 (F1), 1858 (F2), 1890 (F3), and 1916 (F4). Since each tree covers the period 1916-2015, further

examinations were focused on this time interval.

115 For the determination of $\delta^{13}C_{LM}$ values the modified Zeisel method was used (Greule et al., 2009; Keppler et al., 2004, 2007).

The method is based on the reaction between methyl ethers or esters and hydriodic acid (HI) to form iodomethane (Zeisel,

1885). In a 1.5 ml crimp glass vial, 250 µl HI (57 wt% aqueous solution, Acros (Thermo Fisher Scientific)) were added to the 1-10 mg annually dissected tree rings. The vials were sealed with crimp caps and heated for 30 minutes at 130 °C. Samples were then equilibrated at room temperature (22 °C) for at least 30 minutes before an aliquot of headspace was injected into the

120   gas chromatograph – combustion – isotope ratio mass spectrometry (GC-C-IRMS) analytical system. 10-90 µl of the headspace were injected via an autosampler (A200S, CTC Analytics, Zwingen, Switzerland) with a split injection of 10:1 to the HP 6890 N gas chromatograph (Agilent, Santa Clara, USA). The gas chromatograph was fitted with a DB-5MS, Agilent J&W capillary column (length 30 m, internal diameter 0.25 mm, film thickness 0.5 µm) with an initial oven temperature of 50 °C for 2.9 minutes, ramp at 50 °C per minute to 110 °C. Helium was used as carrier gas at a constant flow rate of 1.8 ml min^{-1}. Using an

125   oxidation reactor (ceramic tube (Al_2O_3), length 320 mm, internal diameter 0.5 mm) with Cu, Ni, and Pt wires inside (activated by oxygen) and a reaction temperature of 960 °C, CH_3I is oxidized to CO_2. Before the CO_2 flows through a GC Combustion III Interface (ThermoQuest Finnigan) into the isotope ratio mass spectrometer (253 Plus 10 kV IRMS, Thermo Fisher Scientific), the accrue water was removed through a semipermeable membrane (NAFION®). A tank of high purity carbon dioxide (carbon dioxide 4.5, Messer Griesheim, Frankfurt, Germany) was used as the monitoring gas. For all values, the delta

130   (δ) notation is used, employing the term Urey (Ur, after H.C Urey, 1948) as the isotope delta value unit (Brand and Coplen, 2012). Hence, 1 mUr equates to 1 ‰.

The $\delta^{13}C_{LM}$ values were normalized considering a two-point calibration and two reference materials, potassium methyl sulfate (HUBG 2) and beech wood (HUBG 4) described by Greule et al. (2019, 2020). $\delta^{13}C_{LM}$ values of HUBG 2 and HUBG 4 were calibrated against international isotope reference material (V-PDB) with an isotopic value of $\delta^{13}C_{VPDB}$ = +1.60 ± 0.12 mUr for

135   HUBG2 (Greule et al., 2019) and $\delta^{13}C_{VPDB}$= -30.17 ± 0.13 mUr for HUBG4 (Greule et al., 2020). Before and after every sixth measurement, HUBG 2 and HUBG 4 were measured alternately. The tree rings of the two cores of F1 were measured as triplicates (n=3). Differences between the triplicates were always less than 1 mUr with an average deviation of 0.08 mUr. The maximum differences between two individual cores of the same tree ranged from 1.54 for F1 to 3.26 mUr for F2. Since each tree is represented by the average of two cores, the variances between the triplicate measurements of F1 are marginal compared

140   to the much larger differences of the two cores of the same tree. Therefore, to drastically reduce analytical costs further tree rings from F2-F4 were analyzed by single measurements.

2.3 Correction of $\delta^{13}C_{LM}$ values for non-climatic environmental factors

Due to anthropogenic burning of fossil fuels, the atmospheric CO_2 concentration is steadily increasing. Since fossil CO_2 has a lighter carbon isotopic composition than the atmosphere, the $\delta^{13}C$ values in atmospheric CO_2 ($\delta^{13}C_{atmos}$) show a prominent downwards trend. This so-called "Suess effect" (Keeling, 1979) describes a decrease in $\delta^{13}C_{atmos}$ value from -6.41 mUr in 1850

145   to a current value of -8.6 mUr in 2020. Consequently, leaf internal CO_2 (ci) is already depleted in ^{13}C and even more ^{12}C can be assimilated in leaf sugars, yielding to more negative $\delta^{13}C_{LM}$ values. As this decline is a non-climate effect, the carbon isotopic composition of tree rings needs to be corrected by adding the differences for each year between the $\delta^{13}C_{atmos}$ and the pre-industrial (-6.41 mUr) to the measured $\delta^{13}C_{LM}$ values (Suess effect corrected values are declined as $\delta^{13}C_{LM\_S}$) (McCarroll

150 and Loader, 2004). Here, the $\delta^{13}C_{atmos}$ series was obtained from McCarroll and Loader (2004) and the Mauna Loa Observatory (Keeling et al., 2005, https://scrippsco2.ucsd.edu/data/atmospheric_co2/mlo.html). Furthermore, the leaf internal ^{13}C discrimination increases with rising CO_2 concentration, as the absolute magnitude of mesophyll and photorespiration decreases (Keeling et al., 2017). It is important to note that there is no pre-defined way to correct $\delta^{13}C$ values of trees due to increasing CO_2 concentrations. However, in our study the Suess effect corrected $\delta^{13}C_{LM\_S}$ values were multiplied considering a correction

155 factor per increasing CO_2 parts per million by volume (ppmv) compared to the pre-industrial CO_2 concentration. We used the CO_2 series from MacFarling Meure (2006) and the Global Monitoring Laboratory NOAA (https://gml.noaa.gov/ccgg/trends/;https://scrippsco2.ucsd.edu/). Different studies proposed diverse correction factors. For instance, Kürschner (1996) suggested a correction value of 0.0073 mUr ppmv CO_2^{-1}, Treydte et al. (2009) of 0.012 mUr ppmv CO_2^{-1}, Wang et al. (2011) of 0.016 mUr ppmv CO_2^{-1}, Feng and Epstein (1995) of 0.02 mUr ppmv CO_2^{-1}, and Riechelmann et

160 al. (2016) of 0.032 mUr ppmv CO_2^{-1}. The physiological response due to increasing CO_2 concentration might be different between tree species and locations and is itself a current and important field of study. We additionally detrended the $\delta^{13}C_{LM}$ data using 30-year cubic smoothing splines to emphasize high-frequency variations and evaluate the effects of autocorrelation in our analyses. The resulting $\delta^{13}C_{LM\_high-frequency}$ data were compared with (30-year spline) detrended temperature data to ensure that significant correlations are not simply related to warming trend prevailing over the last 60 years (Fig. 1a).

165 **2.4 Correction of δ^2H_{LM} values considering new reference material**

The δ^2H_{LM} values of trees from Hohenpeißenberg presented by Anhäuser et al. (2020) were normalized using two CH₃I reference standards. As CH₃I is a different material compared to wood and the two CH₃I reference standards did also not cover the entire range of the δ^2H_{LM} values of the samples (-295 to -224 mUr), this study applied the newly available reference material investigated and recommended by Greule et al. (2019 and 2020). Thus, previously measured δ^2H_{LM} values were corrected

170 using the suggested equation of Greule et al. (2021) (Eq. 2). Accordingly, the corrected data shifts the previous δ^2H_{LM} series to more positive values and the differences between previous and corrected δ^2H_{LM} series become larger with decreasing δ^2H_{LM} values.

$$\delta^2H_{LM\_corrected}[mUr] = (\delta^2H_{LM}[mUr] * 0.78) - 45.71 \text{ mUr} \tag{2}$$

Please note, that the previous δ^2H_{LM} chronology of Anhäuser et al. (2020) included nine cores. F1 was represented by three

175 cores and F2-F4 by two cores. To have the same number of replicates of all four trees (n=2) one core from tree F1 was removed.

2.5 Climate data and statistics

The sensitivity of $\delta^{13}C_{LM}$ and δ^2H_{LM} chronologies to climate was assessed by comparisons the mean $\delta^{13}C_{LM}$ and δ^2H_{LM} anomalies as deviations from the 1961-1990 mean with monthly resolved temperatures and precipitation data from a nearby grid point at 47.75°N and 11.25°E as well as large-scale gridded temperatures using the latest CRU TS version 4.04 via the

180 KNMI climate explorer (Harris et al., 2020; Trouet and Jan van Oldenborgh, 2013). For correlations with detrended $\delta^{13}C_{LM\_low-frequency}$ values, low-frequency variances from the temperature data were removed using 30-year cubic smoothing

spline. Correlations among the $\delta^{13}C_{LM}$ and δ^2H_{LM} tree-ring series and between climate parameters and isotope chronologies were calculated over the period 1916 to 2015 using Bravais Person (r). Temporal changes between proxies and climate parameters were assessed using 31-year running correlations. Here, p values < 0.05 were considered significant, and p < 0.001

185   highly significant. The reconstructions skills of $\delta^{13}C_{LM}$ and $\delta^{13}C_{LM\_high\text{-}frequency}$ chronologies were assessed using Durbin-Watson statistics (DW) testing lag-1 autocorrelation in the linear model residuals, the reduction of error (RE), and coefficient of efficiency (CE) statistics. Any positive values of RE and CE are indicative of adequate skills in the reconstructions (Briffa et al., 1988; Cook et al., 1994). All data analyses, statistics, and graphs were calculated and plotted using the software Arstan, OriginPro 2021, and R.

190   **3 Results**

3.1 $\delta^{13}C_{LM}$ values, correction for the Suess effect and physiological response

The $\delta^{13}C_{LM}$ values of the four tree series range from -32.66 to -26.02 mUr from 1916 to 2015 (Fig. 2a). The $\delta^{13}C_{LM}$ anomalies (deviations from the 1961-1990 mean) range from -3.18 to 3.34 mUr with a standard deviation $\sigma = -0.05 \pm 1.05$ mUr (Fig. 2b). The data are characterized by relatively low inter-series correlation (Rbar) of r = 0.23 (p > 0.05) and include a systematic

195   change in coherency over time as indicated by 31-year moving Rbar values. Rbar reaches an average r of 0.24 at the beginning of the chronology between 1916-1939, followed by a rapid decrease to minimum values of r = 0.02 in 1948 and a gradual increase to maximum r = 0.23 in 1995 (Fig. 2c).

The mean $\delta^{13}C_{LM}$ chronology comprises four trees with two cores each over the past 100 years (Fig. 3 black solid line) and is characterized by two phases. From 1916-1965 the chronology includes a minor positive trend of 0.006 mUr year^{-1}, followed

200   by a negative linear trend of -0.02 mUr year^{-1} from 1966-2015 (Fig. 3 dashed lines). After the correction of the Suess effect, the mean $\delta^{13}C_{LM\_S}$ values are less negative and shifted by +0.3 mUr in 1916 and +2.04 mUr in 2015 (Fig. 3 yellow line). Applying additional corrections that account for physiological response due to increasing atmospheric CO_2 concentrations, the $\delta^{13}C_{LM}$ values further increase to more positive values. This effect is particularly visible in the second half of the 20th century until today and clearly depends on the value that has been used as the correction factor (Fig. 3 pink, red, and green line). This

205   study used a wide range of the already applied correction factors of Treydte et al. (2009) ($\delta^{13}C_{LM\_T}$), Feng and Epstein (1995) ($\delta^{13}C_{LM\_FE}$), and Riechelmann et al. (2016) ($\delta^{13}C_{LM\_RL}$). After the correction of the Suess effect, Rbar values initially decreasing from 0.25 for uncorrected $\delta^{13}C_{LM}$ values to 0.16. The highest inter-series correlations were recorded for the $\delta^{13}C_{LM\_RL}$ series (r = 0.55, p < 0.001), as the applied correction factor added the strongest positive trend to the data. The effect of autocorrelation on Rbar values is mitigated in the 30-year high pass filtered data ($\delta^{13}C_{LM\_high\text{-}frequency}$). Mean Rbar reduces to 0.22 and the lag-

210   1 autocorrelation decreases from 0.652 for the uncorrected $\delta^{13}C_{LM}$ to 0.046 for $\delta^{13}C_{LM\_high\text{-}frequency}$ series. Moving Rbar values of the $\delta^{13}C_{LM\_high\text{-}frequency}$ indices show a similar trend than the inter-series correlations of the low-frequency series, characterized by a strong depression between 1940-1966 (Fig. 2c dashed line).
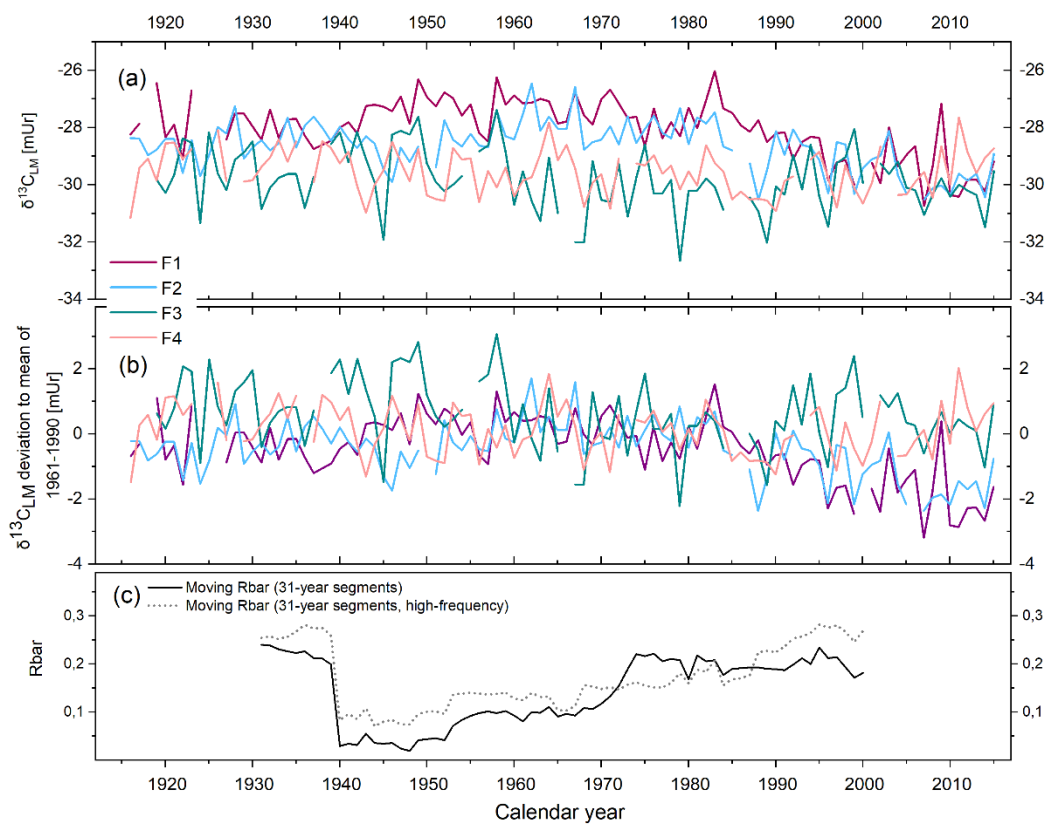
Figure 2. $\delta^{13}C_{LM}$ **series of four Fagus sylvatica trees (F1-F4) from 1916-2015. (a) Annually resolved** $\delta^{13}C_{LM}$ **values. (b)** $\delta^{13}C_{LM}$ **anomalies shown as deviations from the 1961-1990 mean. (c) Moving Rbar of the low- and high-frequency isotope data series.**
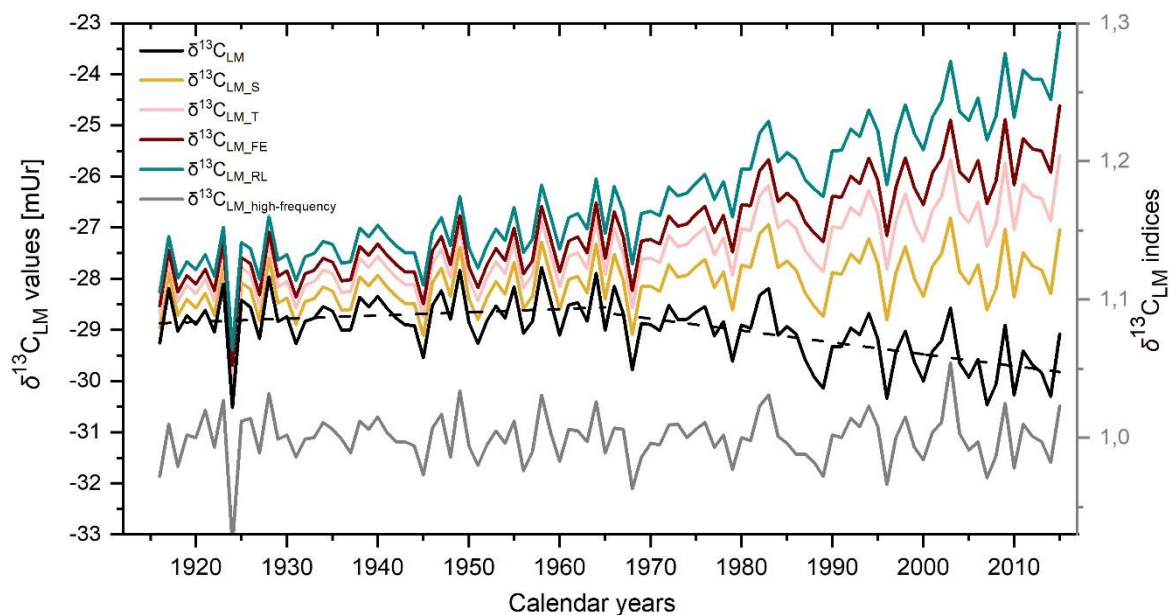
Figure 3. The mean $\delta^{13}C_{LM}$ chronology (black line). Dashed lines show the linear trends until 1965 and from 1965 to 2015. $\delta^{13}C_{LM\_S}$ is the chronology after the corrections of the Suess effect, $\delta^{13}C_{LM\_T}$ after additional correction of physiological response due to increasing CO_2 concentration with $\delta^{13}C_{LM\_T}$ considering 0.012 mUr ppmv^{-1} CO_2, $\delta^{13}C_{LM\_FE}$ considering 0.02 mUr ppmv^{-1} CO_2, and
220   **$\delta^{13}C_{LM\_RL}$ considering 0.032 mUr ppmv^{-1} CO_2. The grey curve shows the detrended $\delta^{13}C_{LM\_high-frequency}$ indices.**

3.2 Climate sensitivities of $\delta^{13}C_{LM}$ chronologies

When comparing $\delta^{13}C_{LM}$ chronologies with climate data, we find positive correlations with regional temperatures and largely non-significant correlations with precipitation. The coefficients tend to increase when considering $\delta^{13}C_{LM}$ chronologies that were corrected for the Suess effect ($\delta^{13}C_{LM\_S}$) and physiological response due to increasing atmospheric CO_2 concentrations

225   ($\delta^{13}C_{LM\_T} < \delta^{13}C_{LM\_FE,} < \delta^{13}C_{LM\_RL}$) (Fig. 4 and S1). Highest correlation coefficients were found between $\delta^{13}C_{LM}$ values and summer (JJA) temperatures ($\delta^{13}C_{LM\_S}$: r = 0.52 to $\delta^{13}C_{LM\_RL}$: r = 0.68) (p < 0.001; the degrees of freedom were reduced, due to lag-1 autocorrelation), followed by MAT ranging from r = 0.42 to 0.66, and 'shifted' annual temperatures (previous September to August) ranging from r = 0.34 to 0.61. Among the mainly non-significant correlations with precipitation totals, the highest coefficient was identified with the just Suess effect corrected $\delta^{13}C_{LM\_S}$ chronology and summer precipitation

230   (r = -0.33)
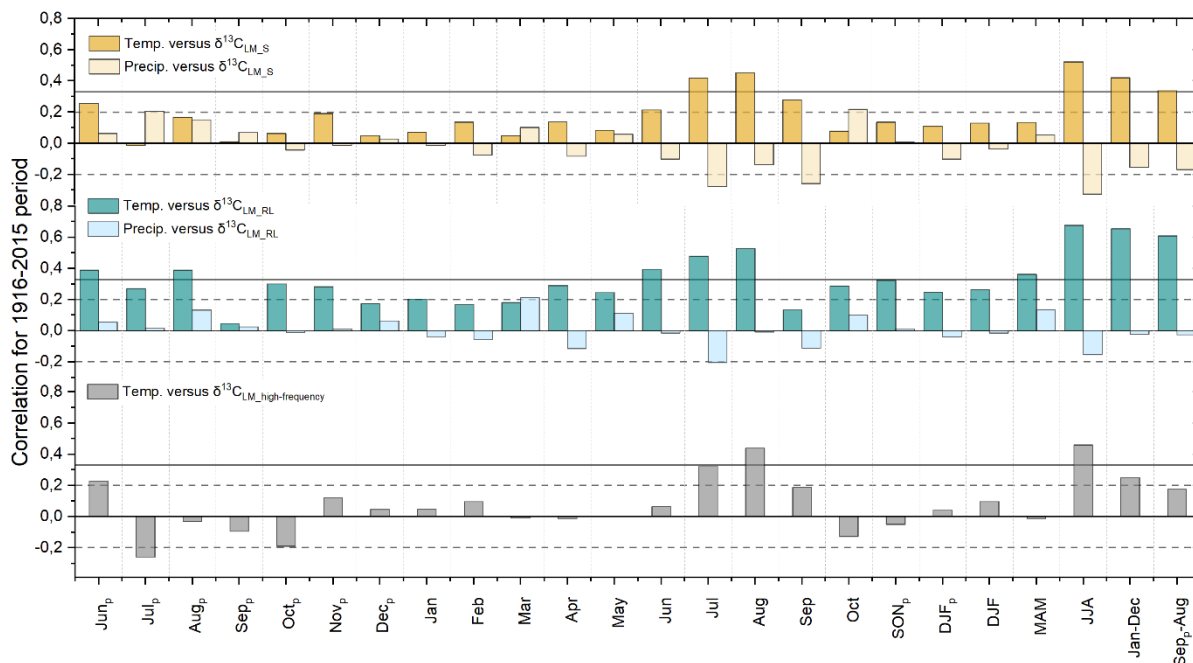
Figure 4. Correlation coefficients between corrected $\delta^{13}C_{LM\_S}$, $\delta^{13}C_{LM\_RL}$, $\delta^{13}C_{LM\_high-frequency}$ chronologies and local temperatures and precipitation totals from 1916 to 2015. The subscript p indicates the months of the previous year, and horizontal lines indicate the significance levels, with solid lines representing highly significant (p < 0.001) and dashed lines representing significant values (p < 0.05).

Additional assessments of climate signals using 30-year high-pass filtered chronologies revealed that correlations with summer temperatures decrease to r = 0.46 but are still significant at p < 0.001. The correlation coefficient with MAT (Jan-Dec) is lower with r = 0.25 (p < 0.05) and non-significant with shifted MAT (Sep_p-Aug) (r = 0.18, p > 0.05).

Since the ideal correction factor was determined by considering summer temperatures as the best fit climate parameter, further relationships with large-scale seasonal temperatures were modelled with $\delta^{13}C_{LM\_RL}$ values (https://climexp.knmi.nl/start.cgi). The patterns extend from southern Europe to middle Scandinavia and cover the UK and western Poland, Slovakia, and Hungary. Here, the highest correlations with r > 0.6 were found between the $\delta^{13}C_{LM\_RL}$ values and summer temperatures in southern Germany, Austria, northern Italy, and northeastern Spain. Followed by somewhat lower correlations of r > 0.5 with summer temperatures in middle Germany, Switzerland, and France and with fall temperatures in northeastern Spain (Fig. 5, S2). Correlations with winter and spring temperatures are always r < 0.5 (S2). Highest correlation between the $\delta^{13}C_{LM\_high-frequency}$ chronology and large-scale summer temperatures extend from southeastern Germany to middle France and cover Switzerland and northern Italy with r > 0.4.
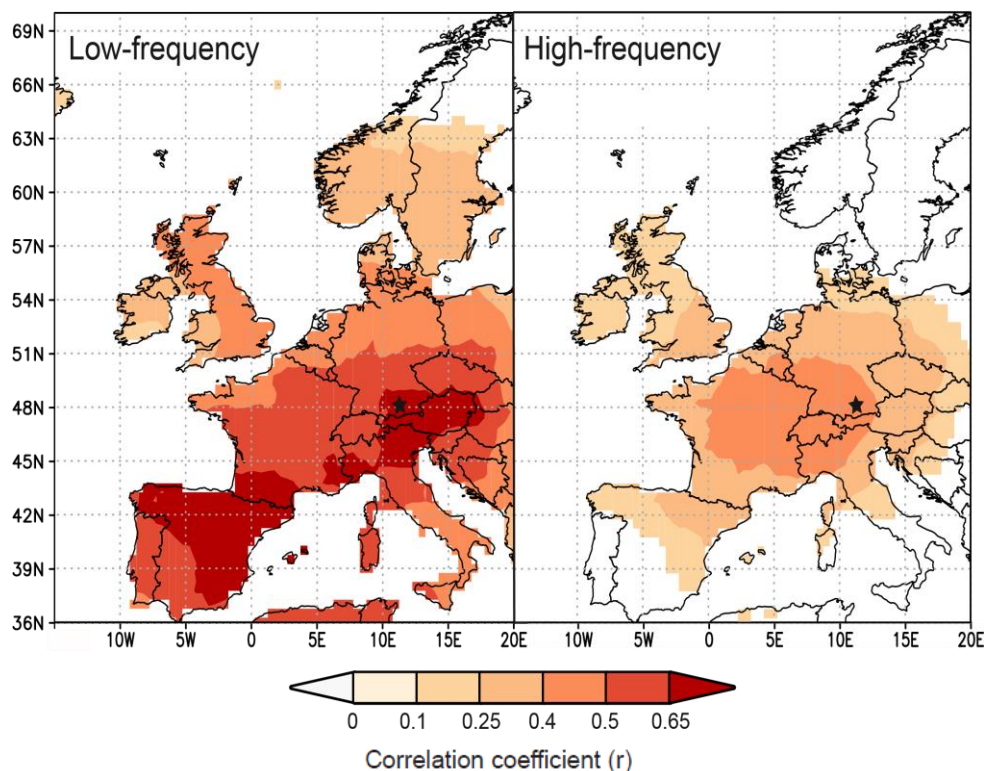
Figure 5. Spatial correlations between summer temperatures (CRU TS4.04) and $\delta^{13}C_{LM\_RL}$ anomalies (left site) and $\delta^{13}C_{LM\_high-frequency}$ indices (right site) from 1916-2015. Black star marks the Hohenpeißenberg in Germany.

3.3 Running correlations and transfer function

The local summer temperatures were modelled by $\delta^{13}C_{LM\_RL}$ values using a linear regression model following Eq. 3.

$$[°C] = \frac{\delta^{13}C \ [mUr] + 0.36}{0.83 \ [mUr \ °C^{-1}]} \qquad (3)$$

$$[°C] = \frac{\delta^{13}C \ [mUr] - 1.29}{-0.29 \ [mUr \ °C^{-1}]} \qquad (4)$$

The regression model residuals ranging between -2.13 to 1.91 and show an increasing trend of 0.022 ± 0.002 over the past 100 years. Between 1916-1963 residuals are mainly negative, whereas since 1964 residuals are mainly positive (Fig. 6a,b). Furthermore, we calculated the Durbin-Watson (DW) statistic of the regression model residuals and reveal a weak DW value of 0.86 which indicates a strong positive autocorrelation ($p < 0.001$). If two series are autocorrelated, the effective sample size and thus the degrees of freedoms may be reduced. Since the significance of the correlation coefficient depends on the degrees of freedoms, significant correlations may well be non-significant under the consideration of autocorrelation (Wigley et al., 1987).

Running correlations between gridded instrumental and modelled regional summer temperatures reveal substantial temporal changes. The 31-year moving correlation values ranging from 0.03 to 0.09 with an average of $r = 0.03 \pm 0.02$ between 1939 to

265   1965. Before 1939, correlation coefficients range from 0.18 to 0.36 with an average r = 0.25 ± 0.07 (p < 0.05). After 1965, correlation values increase rapidly with r ranging from 0.23 to 0.84 (average r = 0.66 ± 0.13 (p < 0.001)) (Fig. 7).

To eliminate the effect of autocorrelation and to constrain high-frequency variations we employed $\delta^{13}C_{LM\_high\text{-}frequency}$ indices for modelling summer temperatures using Eq. 4. The high-frequency chronology reveals a DW value of the regression residuals close to the optimum value of 2 (DW = 2.3) suggesting the robustness of the high-frequency signal. The residuals ranging

270   between -0.04 and 0.07 and show no trend over the 1916-2015 period (Fig. 6c,d).

To determine the strength of the relationship between modelled and observed temperatures we calculated the reduction of error (RE) and coefficient of efficiency (CE) statistics after Cook et al. (1994).

When conducting a split calibration/verification on the high-frequency linear model, a rather weak temporal robustness is indicated (calibration period 1970-2015: RE = -1.67 and CE = -1.68, calibration period 1916-1968: RE = -4.73 and CE = -4.75).

275   To explore this issue in more detail, we calculated 31-year moving correlations between gridded instrumental and modelled summer temperature indices. Running correlations showed significant values at the beginning of the chronology, followed by decreasing correlations to r= 0.04 in 1944 and a gradual increase toward r = 0.76 in 1990 (Fig. 7). Hence, summer temperatures are mainly significantly represented in $\delta^{13}C_{LM\_high\text{-}frequency}$ indices. However, between 1935 to 1954, moving correlations are non-significant. Recalculating the RE and CE statistics for only the 1956 to 2015 period. RE and CE values substantially

280   increase and are close to zero (calibration period: 1986-2015: RE = -0.19 and CE = -0.19 calibration period 1956-1985: R = -0.54 and CE = -0.54).
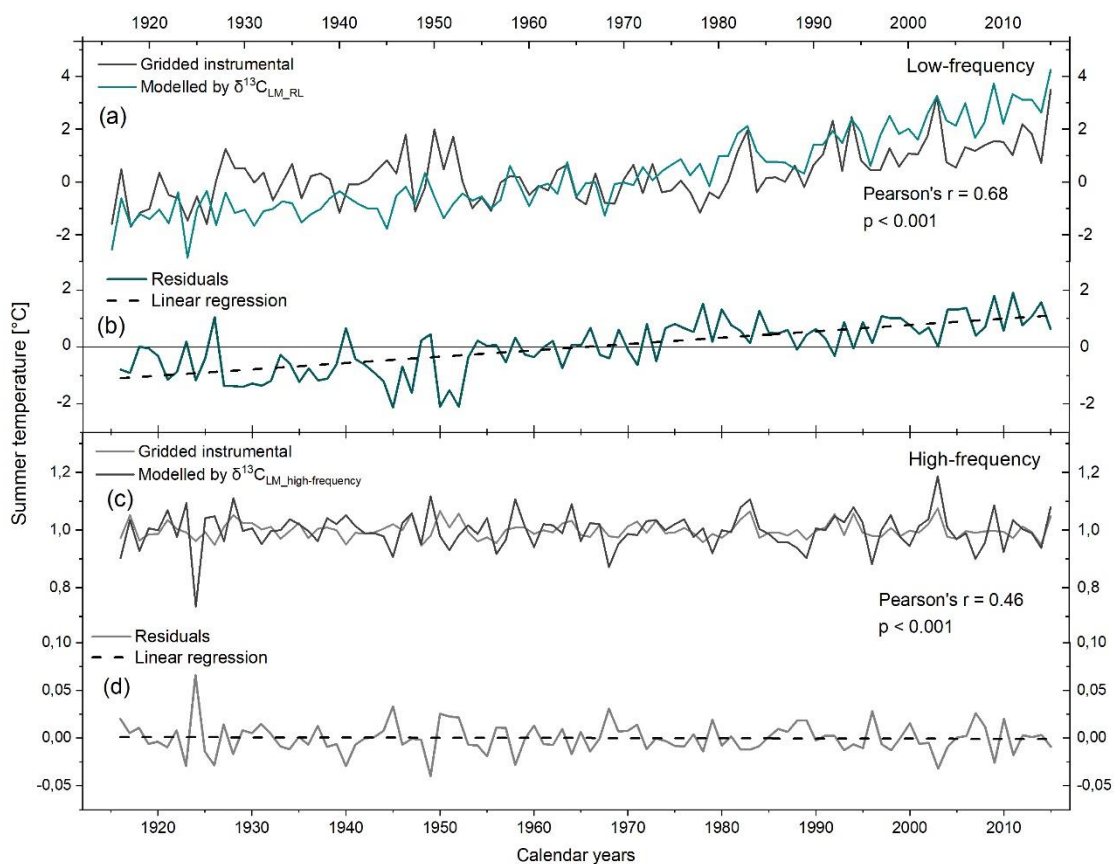
Figure 6. Gridded instrumental and modelled JJA temperatures by (a) $\delta^{13}C_{LM\_RL}$ values and (c) $\delta^{13}C_{LM\_high\text{-}frequency}$ indices from 1916-2015. (b) and (d) plots of residual trends through time for low- and high-frequency.
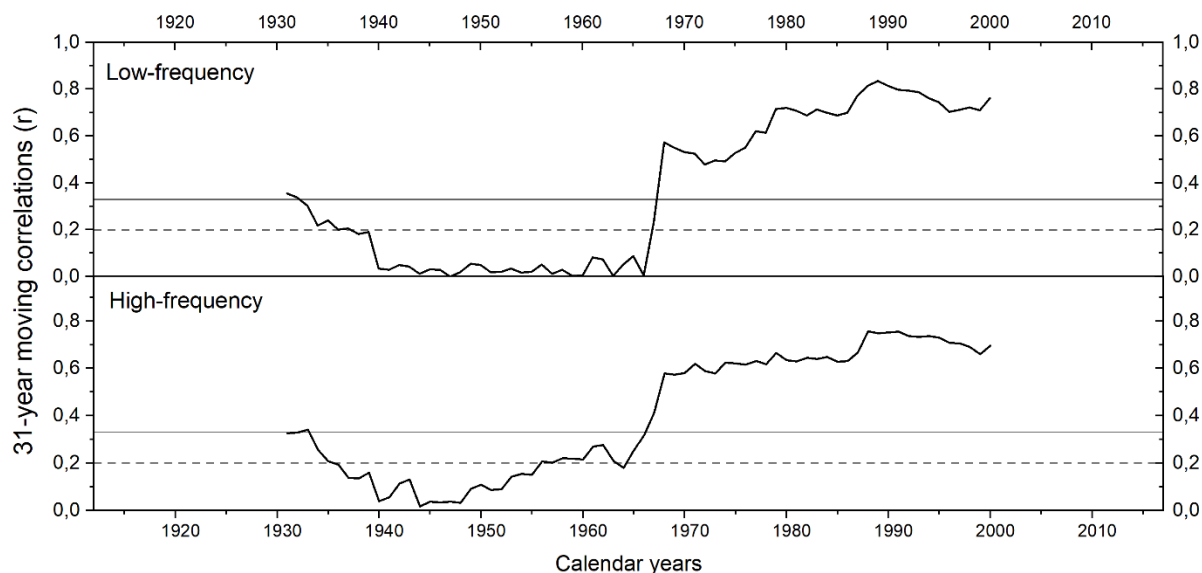
Figure 7. 31-year moving correlations between low- (top panel) and high-frequency (bottom panel) gridded instrumental and modelled summer temperatures.

3.4 $\delta^2 H_{LM}$ chronology and climate signal

290   The $\delta^2 H_{LM}$ values of the tree cores from Hohenpeißenberg previously presented by Anhäuser et al. (2020) were corrected using the relationship provided by Greule et al. (2021) (see Materials and Methods). The revised data showed maximum and minimum $\delta^2 H_{LM}$ values ranging from -274 to -221 mUr around a mean value of -246 ± 9 mUr (1σ standard deviation) and maximum and minimum $\delta^2 H_{LM}$ anomalies from -12.3 to 19.4 with a mean value of 1.9 ± 6.4 mUr. Considering the chronologies of the four trees a highly significant inter-series correlation of r = 0.33 (p < 0.001) can be reported, whereby somewhat higher

295   Rbar values are observed between single radii of the same tree ranging from 0.57 to 0.8. Figure 8 (solid black line) shows the mean $\delta^2 H_{LM}$ chronology of the four trees over the past 100 years. A linear increasing trend of 0.14 mUr year^{-1} is observed over the whole period from 1916-2015, but it is also obvious that the trend is more positive (0.38 mUr year^{-1}) since 1970.
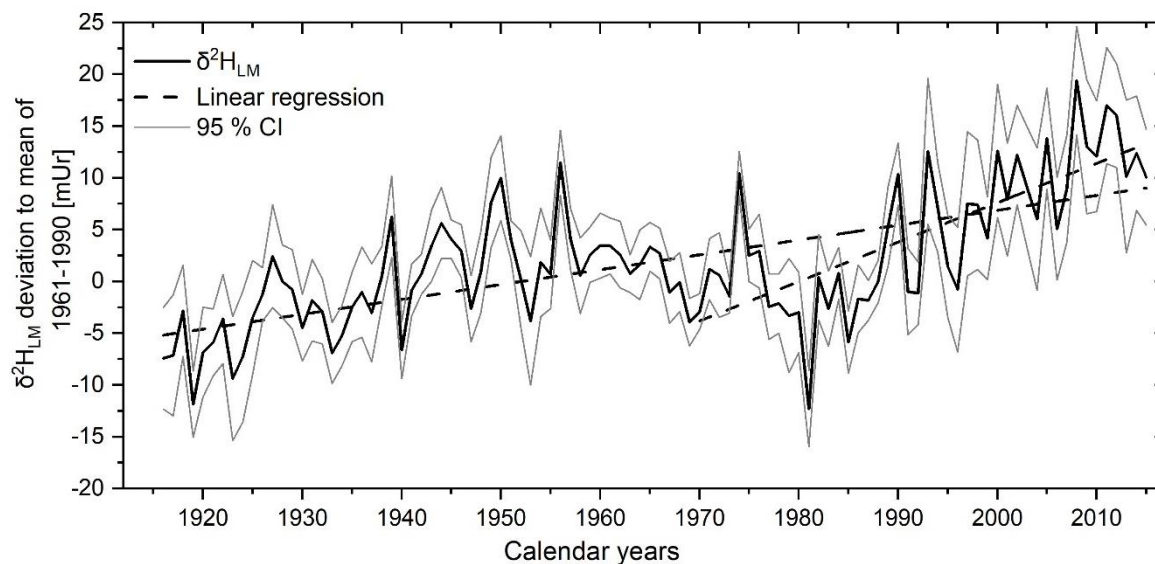
Figure 8. The corrected mean δ^2H_{LM} anomalies as deviations from the 1961-1990 mean from 1916-2015. The 100-year record (black line) represents the mean of the eight individual tree ring series with 95 % CI (grey lines). Linear regression lines (dashed) are shown for the whole period and from 1970-2015.

Highest r values between the corrected δ^2H_{LM} anomalies and temperature are recorded for the 'shifted' annual temperatures (Sep$_p$-Aug) with r = 0.58 (p < 0.001) and the MAT (Jan-Dec) with r = 0.57 (p < 0.001). Furthermore, summer temperatures and δ^2H_{LM} values also showed a highly significant correlation of r = 0.51 (p < 0.001), whereas correlations with winter and previous fall decrease (r = 0.31 and r = 0.3). Correlation coefficients with precipitation were non-significant (p > 0.05). Similar to the results of Anhäuser et al. (2020), the highest correlations were documented with large-scale western European temperatures (r = 0.69) averaged of the region from 15W-20E and 25-75 N (Fig. 9).
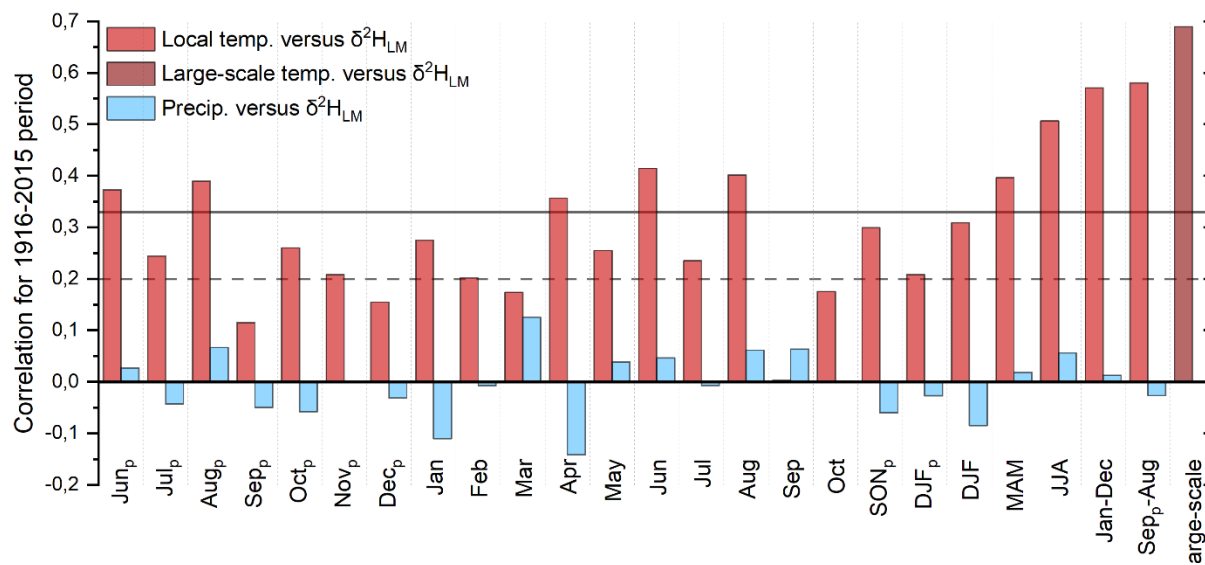
Figure 9. Correlation coefficients between the δ^2H_{LM} chronology, local and large-scale temperatures, and local precipitation amounts
310   from 1916-2015. The subscript p indicates the months of the previous year, and the horizontal lines indicate the significance levels, with solid lines representing highly significant (p < 0.001) and dashed lines representing significant values (p < 0.05).

3.5 Comparison of $\delta^{13}C_{LM}$ and δ^2H_{LM} chronologies

The δ^2H_{LM} chronology correlates negatively with the uncorrected $\delta^{13}C_{LM}$ chronology (r = -0.36), but the coefficients change to positive when comparing with the $\delta^{13}C_{LM}$ chronology that was corrected for the Suess effect (r = 0.29) and increase
315   substantially with the chronology that was additionally corrected for the physiological response ($\delta^{13}C_{LM\_T}$: r = 0.52 to $\delta^{13}C_{LM\_RL}$: r = 0.62). The driver for these changes is the common warming trend now inherent in both isotopic records. The correlations are incoherent over time, however considering the $\delta^{13}C_{LM\_RL}$ chronology, lowest and non-correlations were found between 1940-1953, 1959-1964, and 1975-1981 (Fig. 10). The highest correlations were observed since 1980 when r values gradually increased from a mean of r = 0.13 during 1975-1981 to r = 0.6 during 1990-2000. Importantly during the 1975-1986
320   period, δ^2H_{LM} anomalies decrease while $\delta^{13}C_{LM\_RL}$ anomalies constantly increase.

Comparing the potential application of $\delta^{13}C_{LM}$ and δ^2H_{LM} series as climate proxies, it can be shown that $\delta^{13}C_{LM\_RL}$ values are more affected by regional temperature changes than δ^2H_{LM} values. The sum of correlation coefficients shown in Fig. 4 and 9 considering regional temperature, reached r = 7.91 for $\delta^{13}C_{LM\_RL}$ values and only r = 7.12 for δ^2H_{LM} values. However, comparing δ^2H_{LM} values with large-scale western European 'shifted' annual temperatures, correlations are substantially higher
325   at r = 0.69. For both isotopic elements, weak and mostly non-significant correlations are recorded with precipitation data.
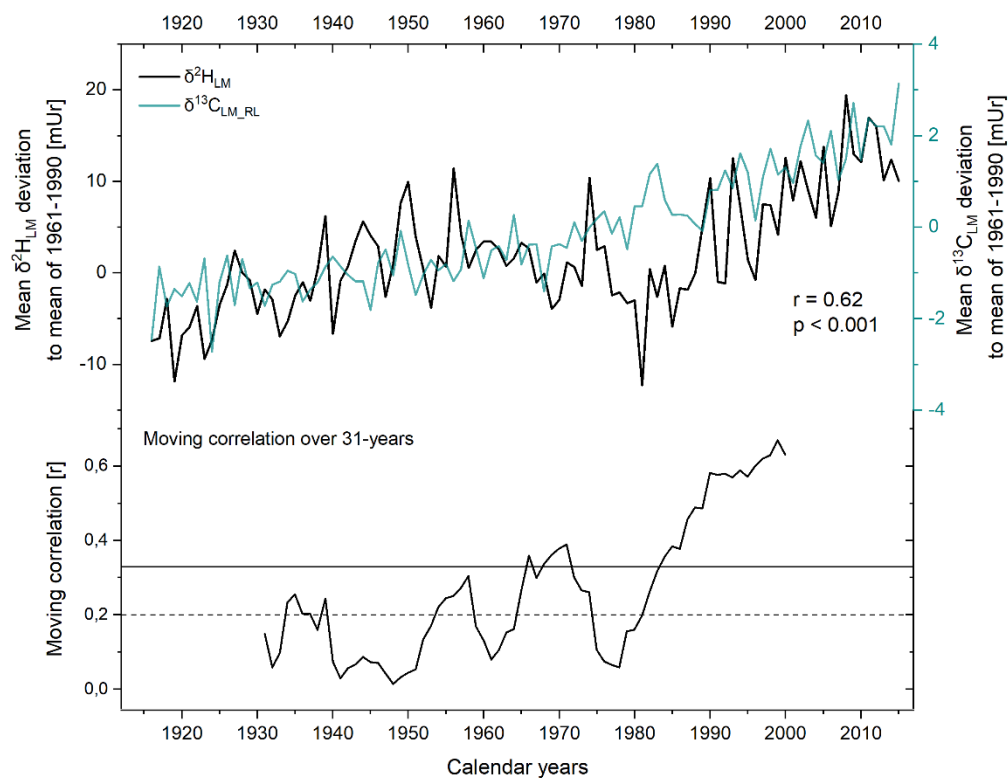
Figure 10. Relationship between annually resolved $\delta^{13}C_{LM\_RL}$ and δ^2H_{LM} chronologies expressed as anomalies relative to the 1961-1990 means. Bottom panel shows the 31-year moving correlations between the isotope chronologies.

4 Discussion

4.1 $\delta^{13}C_{LM}$ values, corrections for non-climate related trends

The average inter-series correlations changes from the uncorrected (r = 0.23), Suess effect corrected (r = 0.16) to the maximum physiological response corrected (r = 0.55) $\delta^{13}C_{LM}$ values as they are influenced by different trend changes (Riechelmann et al., 2016). The correction procedure of the Suess effect removes the prevailing long-term decrease from $\delta^{13}C_{LM}$ values, and the correction for the physiological response produces a positive long-term trend.

Our results showed that the incremental application of corrections for non-climate related trends not only increases the inter-series correlation among trees but also improves the climate correlations. Correlation coefficients with temperature increase significantly by adding a correction factor that accounts for a strong CO_2 response (correlations with $\delta^{13}C_{LM\_T} < \delta^{13}C_{LM\_FE} < \delta^{13}C_{LM\_RL}$). Hence, considering summer temperature as the target climate parameter, the ideal correction factor for *Fagus sylvatica* at this site is 0.032 mUr ppmv^{-1} as introduced by Riechelmann et al. (2016). This factor is also the strongest factor among published and suggests that $\delta^{13}C_{LM}$ values of trees growing in low elevation environments might contain a strong response to increasing CO_2 concentrations. The higher discrimination of ^{13}C by *Fagus Sylvatica* might be related to a lower

water use efficiency of deciduous trees compared to evergreen conifer species (Riechelmann et al., 2016). It has been shown that the studies by Feng and Epstein (1995) and Treydte et al. (2009) mainly used evergreen conifer species and therefore required lower correction factors.

4.2 Climate sensitivity of δ¹³C$_{LM}$ values

345

The greatest climate response was documented between $\delta^{13}C_{LM}$ values and summer temperatures. Here, the strongest relationship was found with the ideal corrected $\delta^{13}C_{LM\_RL}$ chronology (r = 0.68) (Fig. 4). Since correlations with seasonal large-scale temperatures (western European surface temperatures) also showed the highest correlations with summer temperatures in the surrounding area of the study site (Fig. 5), $\delta^{13}C_{LM\_RL}$ values seem to reflect local temperature variations better than large-scale fluctuations.

350

The strong temperature and weak precipitation response indicates that $\delta^{13}C_{LM}$ ratios are predominantly controlled by the photosynthetic rate (McCarroll and Loader, 2004). Similar findings were reported in previous studies applying stable carbon isotopes of tree rings (Gagen et al., 2006; McCarroll and Pawellek, 2001; Riechelmann et al., 2016; Treydte et al., 2009). However, most of these studies analyzed trees from cold, moist, high latitude or high elevation sites. Here, we now demonstrate that local temperatures also strongly influence the $\delta^{13}C_{LM}$ ratios of trees growing in mid-latitude low elevation environments and thus, less extreme conditions.

355

Summer temperature as the controlling factor of $\delta^{13}C_{LM}$ ratios at the Hohenpeißenberg site seems to be intensified in the last 50 years, since moving correlation coefficients between gridded instrumental and modelled records substantially increase after 1966 (Fig. 7). This change in climate sensitivity is not entirely controlled by the increasing temperature trend recorded over recent decades, as similar correlation changes are recorded when using 30-year high-pass filtered tree ring series ($\delta^{13}C_{LM\_high\text{-}frequency}$) and gridded instrumental data. Similar inferences were reported in the study by Treydte et al. (2009). Here, climate correlations were calculated using high-frequency $\delta^{13}C_{LM}$ series to avoid biases from potentially non-climatic long-term trends.

360

The weak DW statistic and positive trend in the low-frequency regression model residuals is partly influenced by the value that has been set as the correction factor on $\delta^{13}C_{LM}$ values. A change in ¹³C discrimination in early increasing CO_2 concentrations might be stronger than the response after an initial adaptation time (Drake et al., 1997; Treydte et al., 2009). This may lead to lower ¹³C discrimination and a decreasing correction factor. Second, anthropogenic warming increases the drought stress of plants growing in mid-latitude sites. To protect from drought stress, plants reduce stomatal conductance, which might lead to an increase in $\delta^{13}C_{LM}$ values (Büntgen et al., 2021). The modern correction of $\delta^{13}C_{LM}$ values, especially in the last decade, may overcorrect the $\delta^{13}C_{LM}$ values and leads to overrated modelled temperatures. It is thus important to note that there are additional uncertainties beyond the linearity of the physiological response to increasing CO_2 concentrations.

365

370

The correlation coefficients between gridded instrumental and modelled summer temperatures were weak between 1935-1954 and 1939-1965 when using the $\delta^{13}C_{LM\_high\text{-}frequency}$ and $\delta^{13}C_{LM\_RL}$ values, respectively. During this early-to-mid 20th century

375 period the temperature sensitivity seems to be influenced by intra-series inconsistencies. This conclusion is supported by contemporaneous low Rbar values (Fig. 11). Indeed, both chronologies correlate strongly (r = 0.74 for $\delta^{13}C_{LM}$ values and r = 0.54 for $\delta^{13}C_{LM\_high-frequency}$ indices). In this study, however, we used two cores from just four trees each. Irregularities in only one or two trees, such as nutrient, water, or light availability, might massively influenced our mean chronology. Additionally, the study side at Hohenpeißenberg is located in an area strongly influenced by human activities. Therefore, soil

380 sealing or tree clearing may have affected the isotopic series and conceal the temperature signal. Saurer et al. (1997) suggested that local effects such as ozone or the availability of water and nutrient could disturb the climate signal. For example, stressors usually increase the $\delta^{13}C$ values and improvements in growing conditions can be expected to decrease $\delta^{13}C$ values (Saurer et al., 1997).

Calculating the RE and CE statistics without the period of low inter-series correlation, the RE and CE values substantially

385 increase indicating the potential of temperature reconstructions by $\delta^{13}C_{LM}$ values if tree ring series are not influenced by non-significant inter-series correlations. The temporal robustness could be improved in further studies by using more replicates on sample sites with less human activity.
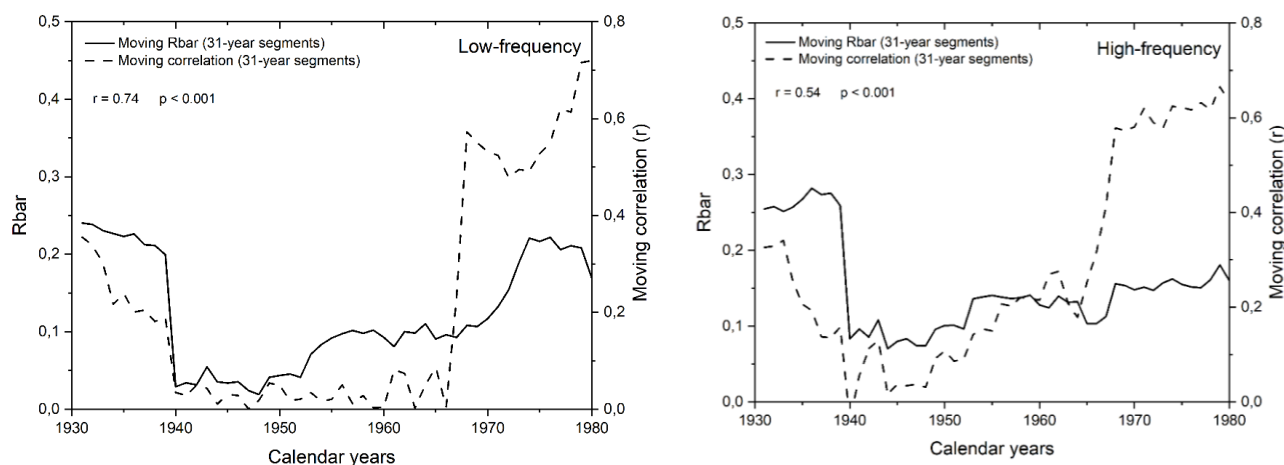
Figure 11. 31-year moving correlations between gridded instrumental and modelled summer temperatures using $\delta^{13}C_{LM\_RL}$ values (left site) and $\delta^{13}C_{LM\_high-frequency}$ indices (right site) (dashed lines) plotted together with the 31-year moving Rbar values of these data (solid lines).

4.3 δ^2H_{LM} values and climate response

The recently provided correction method by Greule et al. (2021) improves the δ^2H_{LM} series of Anhäuser et al. (2020) as a

390 regional temperature proxy. We found a correlation of r = 0.58 with local 'shifted' annual temperatures (Fig. 9), which is slightly higher than the observation of Anhäuser et al. (2020). In addition, we confirm the strong correlation of r = 0.69 with western European surface temperatures as shown by Anhäuser et al. (2020). The increasing long-term trend of the δ^2H_{LM} series clearly reflects the anthropogenic warming trend (slope of 0.14 mUr year^{-1} from 1916-2015). However, a much stronger

increase of 0.38 mUr year^{-1} was found during the most recent period from 1970-2015 (Fig. 8). Interestingly, the ratio between

395   the two slopes of 2.7 is similar to the rates of gridded instrumental temperature changes of 2.4 over these two time periods

(0.015 °C year^{-1} from 1916 to 2015, and 0.036 °C year^{-1} from 1970 to 2015, S3). A possible explanation for the intensified

anthropogenic warming trend in the $\delta^2 H_{LM}$ chronology could be the fact that recent $\delta^2 H_{LM}$ values are additionally controlled

by other environmental factors, such as drought. Strong anthropogenic warming may foster a weaker latitudinal temperature

gradient and therefore a weaker westerly flow, followed by a decreased net terrestrial mid-latitude precipitation (Routson et

400   al., 2019). Büntgen et al. (2021) found generally wetter conditions in the first half of the twentieth century, followed by a

gradual drying trend since the early 1940s. Thus, increasing drought stress for trees growing in the mid-latitudes may have

additionally influenced the intensified $\delta^2 H_{LM}$ trend over the most recent 45 years. This conclusion can be supported by a

comparison of $\delta^2 H_{LM}$ values with summer drought data (self-calibrating Palmer drought severity index) as a tendency toward

increasing negative correlations is recorded since the 1970s (S4, S5).

405   **5 Conclusion**

We measured $\delta^{13}C_{LM}$ values of eight annually resolved 100-year *Fagus sylvatica* tree ring series from the Hohenpeißenberg in

southern Germany and evaluated their sensitivity to climate variations. The $\delta^{13}C_{LM}$ values were corrected for the Suess effect

and the physiological response due to increasing atmospheric CO_2 concentrations using different factors for possible changes

in discrimination. The highest temperature sensitivity was recorded with $\delta^{13}C_{LM}$ values that were corrected for the Suess effect

410   and a correction factor that accounts for a strong CO_2 response of 0.032 mUr ppmv^{-1} ($\delta^{13}C_{LM\_RL}$) as suggested by Riechelmann

et al. (2016). At Hohenpeißenberg, inter-annual to decadal summer temperature variations are significantly reflected in $\delta^{13}C_{LM}$

values. The highest correlation was observed between JJA temperatures and $\delta^{13}C_{LM\_RL}$ values at r = 0.68 (p < 0.001). Lower

but still highly significant correlations were recorded for annual and 'shifted' annual temperatures. To assess the temporal

stability of our tree-ring proxy, summer temperatures were modelled by linearly regressing the $\delta^{13}C_{LM\_RL}$ chronology. Highly

415   significant running correlations particularly over the last 50 years, indicating the potential of $\delta^{13}C_{LM}$ values for reconstructing

summer temperatures at annual resolution. The highly significant correlations between gridded instrumental temperatures and

$\delta^{13}C_{LM\_high\text{-}frequency}$ values confirm the suitability of this proxy to reconstruct high-to-low frequency summer temperatures.

However, our results also indicate that temperature reconstructions based on stable isotope ratios of tree ring lignin methoxy

groups are sensitive to low inter-series correlations. These uncertainties were quantified by evaluating moving Rbar values,

420   RE, and CE statistics and can be improved in further studies by increasing the number of replicate tree samples.

Additional consideration of $\delta^2 H_{LM}$ values from the same trees (Anhäuser et al. 2020; corrected after the suggestion of Greule

et al. 2021) demonstrate that $\delta^2 H_{LM}$ values predominantly reflect large-scale temperatures since highest correlations were found

with western European 'shifted' temperatures (r = 0.69, p < 0.001) and somewhat lower correlations with local 'shifted'

temperature variations (r = 0.58, p < 0.001).

425 The results obtained in this study described for the first time a reliable summer temperature proxy derived from $\delta^{13}C_{LM}$ values in temperate, low elevation environments. We found that $\delta^{13}C_{LM}$ values better preforms with regional and $\delta^{2}H_{LM}$ values with large-scale temperatures, indicating that the two proxies could be combined to reconstruct long-term temperature variations at different spatial and temporal scales.

Data availability

430 We provide the data in heiDATA, which is an institutional repository for research data of the University Heidelberg (https://doi.org/10.11588/data/ZCMVUY).

Author contribution

FK, AW conceived the study. MG performed the measurements and analyzed the data together with FK and AW. JE and PR assisted the application of detrending methods and helped to place the results in a wider dendroclimatological context. The
435 paper was written by FK, AW, JE, PR, and MG. All authors also have given approval to the final version of the manuscript.

Competing interests

The authors declare no competing financial interests.

Acknowledgments

This study was supported by the German Research Foundation DFG (KE 884/6-3, KE 884/8-2, KE 884/17-1). PR received
440 support from the German Research Foundation (Grant No. ES 161/12-1) and JE from ERC Advanced Grant Monostar (AdG 882727) and SustES: Adaptation strategies for sustainable ecosystem services and food security under adverse environmental conditions (CZ.02.1.01/0.0/0.0/16_019/0000797). We are grateful to T. Anhäuser, B. Sehls, B. Knape, C. Hartl, W. Thomas for support in collecting and preparing wood samples.

References

445 Anhäuser, T., Greule, M., Polag, D., Bowen, G. J. and Keppler, F.: Mean annual temperatures of mid-latitude regions derived from δ2H values of wood lignin methoxyl groups and its implications for paleoclimate studies, Sci. Total Environ., 574, 1276–1282, doi:10.1016/j.scitotenv.2016.07.189, 2017a.

Anhäuser, T., Greule, M. and Keppler, F.: Stable hydrogen isotope values of lignin methoxyl groups of four tree species across Germany and their implication for temperature reconstruction, Sci. Total Environ., 579, 263–271, 450 doi:10.1016/j.scitotenv.2016.11.109, 2017b.

Anhäuser, T., Sehls, B., Thomas, W., Hartl, C., Greule, M., Scholz, D., Esper, J. and Keppler, F.: Tree-ring δ2H values from lignin methoxyl groups indicate sensitivity to European-scale temperature changes, Palaeogeogr. Palaeoclimatol. Palaeoecol., 546, doi:10.1016/j.palaeo.2020.109665, 2020.

Brand, W. A. and Coplen, T. B.: Stable Isotope Deltas Tiny yet Robust Signatures in Nature, Heal. Stud., 48, 393–409, 455 https://doi.org/10.1080/10256016.2012.666977, 2012.

Briffa, K. R., Jones, P. D., Pilcher, J. R. and Hughes, M. K.: Reconstructing summer temperatures in northern Fennoscandinavia back to AD 1700 using tree-ring data from Scots pine, Arct. Alp. Res., 20(4), 385–394, doi:10.2307/1551336, 1988.

Büntgen, U., Urban, O., Krusic, P. J., Rybníček, M., Kolář, T., Kyncl, T., Ač, A., Koňasová, E., Čáslavský, J., Esper, J., 460 Wagner, S., Saurer, M., Tegel, W., Dobrovolný, P., Cherubini, P., Reinig, F. and Trnka, M.: Recent European drought extremes beyond Common Era background variability, Nat. Geosci., 14(4), 190–196, doi:10.1038/s41561-021-00698-0, 2021.

Cernusak, L. A., Ubierna, N., Winter, K., Holtum, J. A. M., Marshall, J. D. and Farquhar, G. D.: Environmental and physiological determinants of carbon isotope discrimination in terrestrial plants, New Phytol., 200(4), 950–965, doi:10.1111/nph.12423, 2013.

465 Cook, E. R., Briffa, K. R. and Jones, P. D.: Spatial regression methods in dendroclimatology: A review and comparison of two techniques, Int. J. Climatol., 14(4), 379–402, doi:10.1002/joc.3370140404, 1994.

Dansgaard, W.: Stable isotopes in precipitation, Tellus, 16(4), 436–468, doi:10.3402/tellusa.v16i4.8993, 1964.

Daux, V., Edouard, J. L., Masson-Delmotte, V., Stievenard, M., Hoffmann, G., Pierre, M., Mestre, O., Danis, P. A. and Guibal, F.: Can climate variations be inferred from tree-ring parameters and stable isotopes from Larix decidua? Juvenile effects, 470 budmoth outbreaks, and divergence issue, Earth Planet. Sci. Lett., 309(3–4), 221–233, doi:10.1016/j.epsl.2011.07.003, 2011.

Drake, B. G., Gonzàlez-Meler, M. A. and Long, S. P.: More efficient plants: A Consequence of Rising Atmospheric CO2?, Annu. Rev. Plant Biol., 48, 609–639, doi:10.1146/annurev.arplant.48.1.609, 1997.

Esper, J.: Long-term tree-ring variations in Juniperus at the upper timber-line in the Karakorum (Pakistan), The Holocene, 10, 253–260, https://doi.org/10.1191/095968300670152685, 2000.

475 Esper, J., Konter, O., Krusic, P. J., Saurer, M., Holzkämper, S. and Büntgen, U.: Long-term summer temperature variations in the Pyrenees from detrended stable carbon isotopes, Geochronometria, 42(1), 53–59, doi:10.1515/geochr-2015-0006, 2015.

Esper, J., Krusic, P. J., Ljungqvist, F. C., Luterbacher, J., Carrer, M., Cook, E., Davi, N. K., Hartl-Meier, C., Kirdyanov, A., Konter, O., Myglan, V., Timonen, M., Treydte, K., Trouet, V., Villalba, R., Yang, B. and Büntgen, U.: Ranking of tree-ring based temperature reconstructions of the past millennium, Quat. Sci. Rev., 145, 134–151, 480 doi:10.1016/j.quascirev.2016.05.009, 2016.

Esper, J., Holzkämper, S., Büntgen, U., Schöne, B., Keppler, F., Hartl, C., George, S. S., Riechelmann, D. F. C. and Treydte, K.: Site-specific climatic signals in stable isotope records from Swedish pine forests, Trees - Struct. Funct., 32(3), 855–869, doi:10.1007/s00468-018-1678-z, 2018.

Farquhar, G. D., Leary, M. H. O. and Berry, J. A.: On the Relationship between Carbon Isotope Discrimination and the
485   Intercellular Carbon Dioxide Concentration in Leaves, 9, 121–37, doi:https://doi.org/10.1071/PP9820121, 1982.

Feng, X. and Epstein, S.: Carbon isotopes of trees from arid environments and implications for reconstructing atmospheric CO_2 concentration, Geochim. Cosmochim. Acta, 59(12), 2599–2608, doi:10.1016/0016-7037(95)00152-2, 1995.

Francey, R. J. and Farquhar, G. D.: An explanation of 13C/12C variations in tree rings, Nature, 297(May), 28–31, https://doi.org/10.1038/297028a0, 1982.

490   Gagen, M., McCarroll, D., Loader, N. J., Robertson, I., Jalkanen, R. and Anchukaitis, K. J.: Exorcising the "segment length curse": Summer temperature reconstruction since AD 1640 using non-detrended stable carbon isotope ratios from pine trees in northern Finland, Holocene, 17(4), 435–446, doi:10.1177/0959683607077012, 2006.

Gori, Y., Wehrens, R., Greule, M., Keppler, F., Ziller, L., La Porta, N. and Camin, F.: Carbon, hydrogen and oxygen stable isotope ratios of whole wood, cellulose and lignin methoxyl groups of Picea abies as climate proxies, Rapid Commun. Mass
495   Spectrom., 27(1), 265–275, doi:10.1002/rcm.6446, 2013.

Greule, M., Mosandl, A., Hamilton, J. T. G. and Keppler, F.: A rapid and precise method for determination of D/H ratios of plant mathoxyl groups, Rapid Commun. Mass Spectrom., 22, 3983–3988, doi:10.1002/rcm, 2008.

Greule, M., Mosandl, A., Hamilton, J. T. G. and Keppler, F.: A simple rapid method to precisely determine 13C/12C ratios of plant methoxyl groups, Rapid Commun. Mass Spectrom., 23, 1710–1714, doi:10.1002/rcm, 2009.

500   Greule, M., Moossen, H., Geilmann, H., Brand, W. A. and Keppler, F.: Methyl sulfates as methoxy isotopic reference materials for δ 13 C and δ 2 H measurements, Rapid Commun. Mass Spectrom., 33(4), 343–350, doi:10.1002/rcm.8355, 2019.

Greule, M., Moossen, H., Lloyd, M. K., Geilmann, H., Brand, W. A., Eiler, J. M., Qi, H. and Keppler, F.: Three wood isotopic reference materials for δ2H and δ13C measurements of plant methoxy groups, Chem. Geol., 533(August 2019), 119428, doi:10.1016/j.chemgeo.2019.119428, 2020.

505   Greule, M., Wieland, A. and Keppler, F.: Measurements and applications of d 2 H values of wood lignin methoxy groups for paleoclimatic studies, Quat. Sci. Rev., 268, 107107, doi:10.1016/j.quascirev.2021.107107, 2021.

Hafner, P., Robertson, I., McCarroll, D., Loader, N. J., Gagen, M., Bale, R. J., Jungner, H., Sonninen, E., Hilasvuori, E. and Levanič, T.: Climate signals in the ring widths and stable carbon, hydrogen and oxygen isotopic composition of Larix decidua growing at the forest limit in the southeastern European Alps, Trees - Struct. Funct., 25(6), 1141–1154, doi:10.1007/s00468-
510   011-0589-z, 2011.

Harris, I., Osborn, T. J., Jones, P. and Lister, D.: Version 4 of the CRU TS monthly high-resolution gridded multivariate climate dataset, Sci. Data, 7(1), 1–18, doi:10.1038/s41597-020-0453-3, 2020.

Hepp, J., Zech, R., Rozanski, K., Tuthorn, M., Glaser, B., Greule, M., Keppler, F., Huang, Y., Zech, W. and Zech, M.: Late Quaternary relative humidity changes from Mt. Kilimanjaro, based on a coupled 2H-18O biomarker paleohygrometer approach, Quat. Int., 438, 116–130, doi:10.1016/j.quaint.2017.03.059, 2017.

Keeling, C. D.: The Suess effect: 13Carbon-14Carbon interrelations, Environ. Int., 2(4–6), 229–300, doi:10.1016/0160-4120(79)90005-9, 1979.

Keeling, C. D., Piper, S. C., Bacastow, R. B., Wahlen, M., Whorf, T. P., Heimann, M. and Meijer, H. A.: Atmospheric CO2 and 13CO2 Exchange with the Terrestrial Biosphere and Oceans from 1978 to 2000: Observations and Carbon Cycle Implications, A Hist. Atmos. CO2 Its Eff. Plants, Anim. Ecosyst., 83–113, doi:10.1007/0-387-27048-5_5, 2005.

Keeling, R. F., Graven, H. D., Welp, L. R., Resplandy, L., Bi, J., Piper, S. C., Sun, Y., Bollenbacher, A. and Meijer, H. A. J.: Atmospheric evidence for a global secular increase in carbon isotopic discrimination of land photosynthesis, Proc. Natl. Acad. Sci. U. S. A., 114(39), 10361–10366, doi:10.1073/pnas.1619240114, 2017.

Keppler, F., Kalin, R. M., Harper, D. B., McRoberts, W. C. and Hamilton, J. T. G.: Carbon isotope anomaly in the major plant C1 pool and its global biogeochemical implications, Biogeosciences, 1(2), 123–131, doi:10.5194/bg-1-123-2004, 2004.

Keppler, F., Harper, D. B., Kalin, R. M., Meier-Augenstein, W., Farmer, N., Davis, S., Schmidt, H. L., Brown, D. M. and Hamilton, J. T. G.: Stable hydrogen isotope ratios of lignin methoxyl groups as a paleoclimate proxy and constraint of the geographical origin of wood, New Phytol., 176(3), 600–609, doi:10.1111/j.1469-8137.2007.02213.x, 2007.

Konter, O., Holzkämper, S., Helle, G., Büntgen, U., Saurer, M. and Esper, J.: Climate sensitivity and parameter coherency in annually resolved δ13C and δ18O from Pinus uncinata tree-ring data in the Spanish Pyrenees, Chem. Geol., 377, 12–19, doi:10.1016/j.chemgeo.2014.03.021, 2014.

Kress, A., Saurer, M., Siegwolf, R. T. W., Frank, D. C., Esper, J. and Bugmann, H.: A 350 year drought reconstruction from Alpine tree ring stable isotopes, Global Biogeochem. Cycles, 24(2), 1–16, doi:10.1029/2009GB003613, 2010.

Kürschner, W.M., Leaf Stomata as Biosensors of Palaeoatmospheric CO2 Levels, Utr. Univ., 153p., 1996.

Lee, H., Feng, X., Mastalerz, M. and Feakins, S. J.: Characterizing lignin: Combining lignin phenol, methoxy quantification, and dual stable carbon and hydrogen isotopic techniques, Org. Geochem., 136, 103894, doi:10.1016/j.orggeochem.2019.07.003, 2019.

Ljungqvist, F. C., Piermattei, A., Seim, A., Krusic, P. J., Büntgen, U., He, M., Kirdyanov, A. V., Luterbacher, J., Schneider, L., Seftigen, K., Stahle, D. W., Villalba, R., Yang, B. and Esper, J.: Ranking of tree-ring based hydroclimate reconstructions of the past millennium, Quat. Sci. Rev., 230, 106074, doi:10.1016/j.quascirev.2019.106074, 2020.

MacFarling Meure, C., Etheridge, D., Trudinger, C., Steele, P., Langenfelds, R., Van Ommen, T., Smith, A. and Elkins, J.: Law Dome CO2, CH4 and N2O ice core records extended to 2000 years BP, Geophys. Res. Lett., 33(14), 2000–2003, doi:10.1029/2006GL026152, 2006.

McCarroll, D. and Loader, N. J.: Stable isotopes in tree rings, Quat. Sci. Rev., 23(7–8), 771–801, doi:10.1016/j.quascirev.2003.06.017, 2004.

McCarroll, D. and Pawellek, F.: Stable carbon isotope ratios of Pinus sylvestris from northern Finland and the potential for extracting a climate signal from long Fennoscandian chronologies, Holocene, 11(5), 517–526, doi:10.1191/095968301680223477, 2001.

Mischel, M., Esper, J., Keppler, F., Greule, M. and Werner, W.: δ2H, δ13C and δ18O from whole wood, α-cellulose and lignin

550   methoxyl groups in Pinus sylvestris: a multi-parameter approach, Isotopes Environ. Health Stud., 51(4), 553–568, doi:10.1080/10256016.2015.1056181, 2015.

Van Raden, U. J., Colombaroli, D., Gilli, A., Schwander, J., Bernasconi, S. M., van Leeuwen, J., Leuenberger, M. and Eicher, U.: High-resolution late-glacial chronology for the Gerzensee lake record (Switzerland): δ18O correlation between a Gerzensee-stack and NGRIP, Palaeogeogr. Palaeoclimatol. Palaeoecol., 391, 13–24, doi:10.1016/j.palaeo.2012.05.017, 2013.

555   Reynolds-Henne, C. E., Siegwolf, R. T. W., Treydte, K. S., Esper, J., Henne, S. and Saurer, M.: Temporal stability of climate-isotope relationships in tree rings of oak and pine (Ticino, Switzerland), Global Biogeochem. Cycles, 21(4), 1–12, doi:10.1029/2007GB002945, 2007.

Riechelmann, D. F. C., Greule, M., Treydte, K., Esper, J. and Keppler, F.: Climate signals in δ13C of wood lignin methoxyl groups from high-elevation larch trees, Palaeogeogr. Palaeoclimatol. Palaeoecol., 445, 60–71,

560   doi:10.1016/j.palaeo.2016.01.001, 2016.

Riechelmann, D. F. C., Greule, M., Siegwolf, R. T. W., Anhäuser, T., Esper, J. and Keppler, F.: Warm season precipitation signal in δ2H values of wood lignin methoxyl groups from high elevation larch trees in Switzerland, Rapid Commun. Mass Spectrom., 31(19), 1589–1598, doi:10.1002/rcm.7938, 2017.

Routson, C. C., McKay, N. P., Kaufman, D. S., Erb, M. P., Goosse, H., Shuman, B. N., Rodysill, J. R. and Ault, T.: Mid-

565   latitude net precipitation decreased with Arctic warming during the Holocene, Nature, 568(7750), 83–87, doi:10.1038/s41586-019-1060-3, 2019.

Saurer, M., Borella, S. and Schweingruber, F.: Stable carbon isotopes in tree rings of beech: climatic versus site-related influences, Trees, 11, 291–297, 1997.

Van der Schrier, G., Barichivich, J., Briffa, K. R. and Jones, P. D.: A scPDSI-based global data set of dry and wet spells for

570   1901-2009, J. Geophys. Res. Atmos., 118(10), 4025–4048, doi:10.1002/jgrd.50355, 2013.

Seibt, U., Rajabi, A., Griffiths, H. and Berry, J. A.: Carbon isotopes and water use efficiency: Sense and sensitivity, Oecologia, 155(3), 441–454, doi:10.1007/s00442-007-0932-7, 2008.

Sternberg, L. D. S. L. O. R.: Oxygen stable isotope ratios of tree-ring cellulose: The next phase of understanding, New Phytol., 181(3), 553–562, doi:10.1111/j.1469-8137.2008.02661.x, 2009.

575   Stoffel, M. and Bollschweiler, M.: Tree-ring analysis in natural hazards research - An overview, Nat. Hazards Earth Syst. Sci., 8(2), 187–202, doi:10.5194/nhess-8-187-2008, 2008.

Tang, K., Feng, X. and Ettl, G. J.: The variations in δD of tree rings and the implications for climatic reconstruction, Geochim. Cosmochim. Acta, 64(10), 1663–1673, doi:10.1016/S0016-7037(00)00348-3, 2000.

Treydte, K., Schleser, G., Schweingruber, F. and Winiger, M.: The climatic significance of δ 13 C in subalpine spruces
580   (Lötschental, Swiss Alps) : A case study with respect to altitude, exposure and soil moisture, Tellus B Chem. Phys. Meteorol.,
53(5), 593–611, doi:10.3402/tellusb.v53i5.16639, 2001.

Treydte, K. S., Frank, D. C., Saurer, M., Helle, G., Schleser, G. H. and Esper, J.: Impact of climate and CO2 on a millennium-
long tree-ring carbon isotope record, Geochim. Cosmochim. Acta, 73(16), 4635–4647, doi:10.1016/j.gca.2009.05.057, 2009.

Trouet, V. and Jan van Oldenborgh, G.: KNMI Climate Explorer : A Web-Based Research Tool for, Tree-Ring Res., 69(1), 3–
585   13, 2013.

Urey, H. C.: Oxygen Isotopes in Nature and in the Laboratory, , 108(2810), 489–496, 1948.

Wang, W., Liu, X., Shao, X., Leavitt, S., Xu, G., An, W. and Qin, D.: A 200 year temperature record from tree ring δ13C at
the Qaidam Basin of the Tibetan Plateau after identifying the optimum method to correct for changing atmospheric CO2 and
δ13C, J. Geophys. Res. Biogeosciences, 116(4), 1–12, doi:10.1029/2011JG001665, 2011.

590   Wang, Y., Liu, X., Anhäuser, T., Lu, Q., Zeng, X., Zhang, Q., Wang, K., Zhang, L., Zhang, Y. and Keppler, F.: Temperature
signal recorded in δ2H and δ13C values of wood lignin methoxyl groups from a permafrost forest in northeastern China, Sci.
Total Environ., 727, 138558, doi:10.1016/j.scitotenv.2020.138558, 2020.

Wigley, T. M. L., Jones, P. D. and Briffa, K. R.: Cross-dating methods in dendrochronology, J. Archaeol. Sci., 14(1), 51–64,
doi:10.1016/S0305-4403(87)80005-5, 1987.

595   Zeisel, S.: Über ein Verfahren zum quantitativen Nachweise von Methoxyl., Monatshefte für Chemie, 989–997,
https://doi.org/10.1007/BF01554683, 1885.